Supplementary Material

An Acetate bridged centrosymmetric trinuclear Zn(II) cluster: Structural insights, biomolecular interactions, sensing and cytotoxic activity

Imtiyaz Ahmad Mantoo[a], Masrat Bashir[a], Mushtaq Ahmad Nengroo[b], Shahnawaz Ali Bhat[c], Imtiyaz Yousuf[a]*

[a]*Department of Chemistry, Aligarh Muslim University, Aligarh 202002, Uttar Pradesh, India.*
[b]*Division of Cancer Biology, CSIR−Central Drug Research Institute (CDRI), Lucknow, 226031.*
[c]*Department of Chemistry, Aligarh Muslim University, Aligarh 202002, Uttar Pradesh, India*
*Corresponding author *E–mail address*: imtiyazchem@gmail.com (I. Yousuf)

Tables

Table S1: Experimental and DFT calculated parameters (bond angles and bond lengths) for complex **1.**

Bond angles in Å					
atom−atom	**experimental**	**calculated**	**atom−atom**	**experimental**	**calculated**
Zn1−Zn2	**3.090(4)**	**3.095**	C8−C7	**1.403(4)**	**1.404**
Zn1−O1	**2.168(2)**	**2.160**	C22−C24	**1.492(5)**	**1.492**
Zn1−O2	**2.074(2)**	**2.075**	N13−C14	**1.476(5)**	**1.476**
Zn1−O3	**2.060(2)**	**2.065**	Zn2−N1	**2.016(3)**	**2.014**
Zn2−O4	**2.067(2)**	**2.066**	Zn2−N2	**2.291(3)**	**2.292**
Zn2−O5	**2.102(2)**	**2.110**	C3−C4	**1.418(5)**	**1.421**
Zn2−O3	**2.542(2)**	**2.541**	C3−C9	**1.427(5)**	**1.428**
C8−C3	**1.417(4)**	**1.416**	C6−C5	**1.377(5)**	**1.376**

Table S2: Experimental and DFT calculated parameters (bond angles and bond lengths) for complex **1.**

Bond angles in					
atom−atom−atom	**Experimental**	**Calculated**	**atom−atom−atom**	**Experimental**	**calculated**
Zn2 Zn1 Zn2	180.0	179.7	N13 Zn2O21	82.95(10)	82.97
O1 Zn1 Zn2	138.13(6)	138.2	N13 Zn2N10	82.13(11)	82.17
$O1^1$ Zn1 Zn2	41.87(6)	42.0	Zn2O1Zn1	93.68(8)	93.71
$O1^1$ Zn1 Zn2	138.13(6)	138.09	C22O1Zn1	121.1(2)	121.09
O1 Zn1 Zn2	41.87(6)	41.82	C22O1Zn2	102.8(2)	102.12

Table S3 Energy of various FMOs of **C1** and its respective HOMO−LUMO energy gaps.

FMOs	**Energy (eV)**	**FMOs**	**Energy (eV)**	**ΔE**
HOMO	4.599	LUMO	1.624	2.975
HOMO–1	4.707	LUMO+1	1.531	3.176
HOMO–2	5.348	LUMO+2	0.626	4.722
HOMO 3	5.990	LUMO+3	0.557	5.433

Table S4: Estimation of thermodynamic and reactivity parameters of **C1** by using B3LYP hybrid functional.

Parameters	**C1**
LUMO energy (eV)	−1.624
HOMO energy (eV)	−4.599
LUMO–HOMO	2.975
EA	1.624
IP	4.599
χ(eV)	3.112
μ(eV)	−3.11
η(eV)	1.488
ω(eV)	3.253

Table S5 Cathodic and Anodic potential (mV) and current (A) for the redox couples of **C1** with ct−DNA in 5mM Tris−buffer solution (pH 7.3) at a scan rate of 100mV s^{-1}

	C1 Alone		**C1 + ct−DNA**		ΔE_{pa}	ΔE_{pc}
	Potential (mV)	**Current (A)**	**Potential (mV)**	**Current (A)**		
C1	E_{pa} = 992 E_{pc} = 582 $E_{1/2}$ = 787 ΔE_p = –410	I_{pa} = 1.036 × 10^{-5} I_{pc} = 1.370 × 10^{-5} I_{pa}/I_{pc} = 0.756	E_{pa} = 1012 E_{pc} = 614 $E_{1/2}$ = 813 ΔE_p = −398	I_{pa} = 1.838 × 10^{-5} I_{pc} = 1.556 × 10^{-5} I_{pa}/I_{pc} = 1.18	–20	–32

Table S6 Comparison of the kinetic parameters *viz.,* ***Km***, K_{cat} and V_{max} of trinuclear Zn(II) clusters.

Complex	V_{max} (Ms^{-1})	K_M (M)	K_{cat} (h^{-1})	**Ref.**
$[Zn_3L_2(\mu{-}O_2\ CCH_3)_2(CH_3OH)_4]$	3 × 10^{-3}	1.06 × 10^{-3}	1.33× 10^3	S1
$[Zn_3(L)(NCS)_2](NO_3)_2(CH_3OH)(H_2O)$	2.58 × 10^{-5}	1.88 × 10^{-3}	9.28× 10^2	S2
$[Zn_3L_2(\mu^{1,2}{-}OAc)_2(\mu^{1,1,2}{-}OAc)_2]$	6.0 × 10^{-2}	5.6 × 10^{-3}	8.4 × 10^2	**Current work**

Table S7 Percent inhibition of ascorbic acid (**AA**) and **C1** with DPPH.

Conc.	**AA**	**C1**
5μM	9.45	8.22
10μM	22.23	23.14
15μM	47.56	51.26
20μM	59.63	63.22
25μM	69.45	73.25
30μM	77.23	83.26
35μM	85.25	90.13
40μM	94.56	96.29

Figures

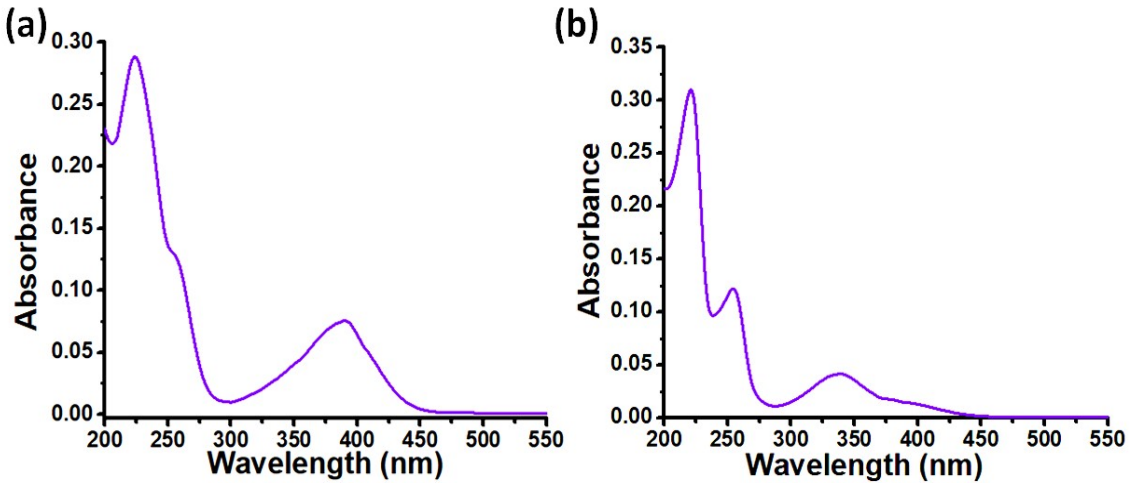

Fig. S1. UV−vis spectra of (a) **L1** and (b) **C1** recorded in MeOH.

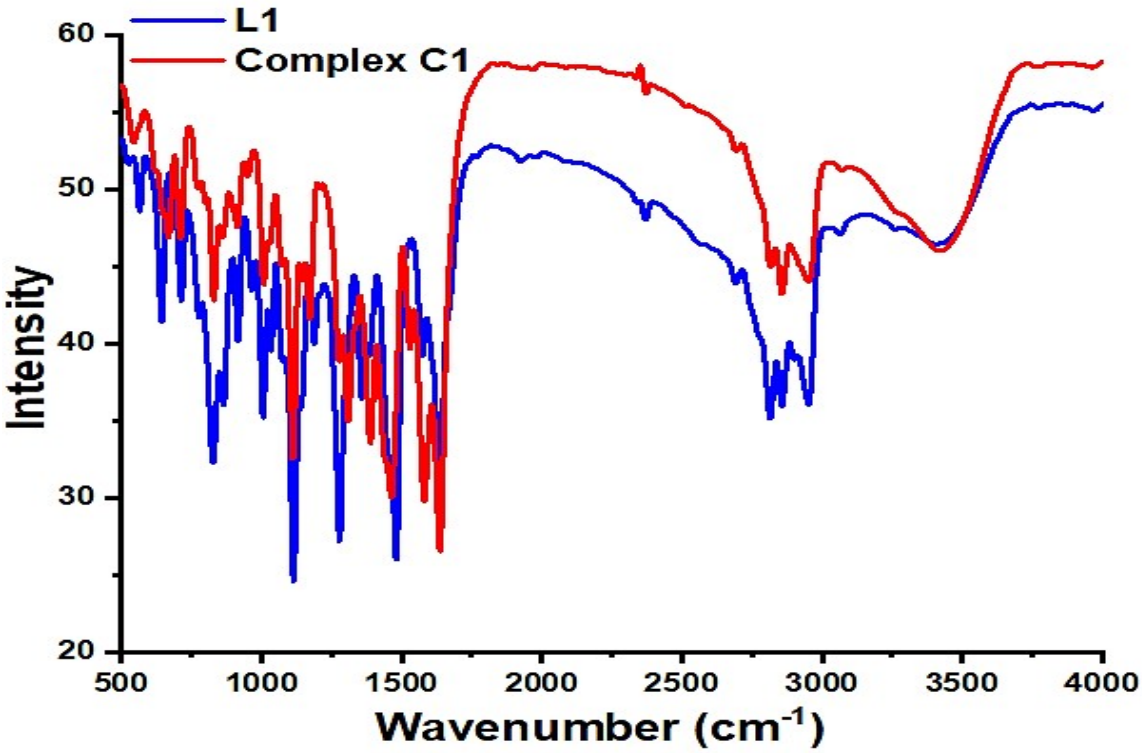

Fig. S2 The comparative FTIR spectral data of **L1** and **C1.**

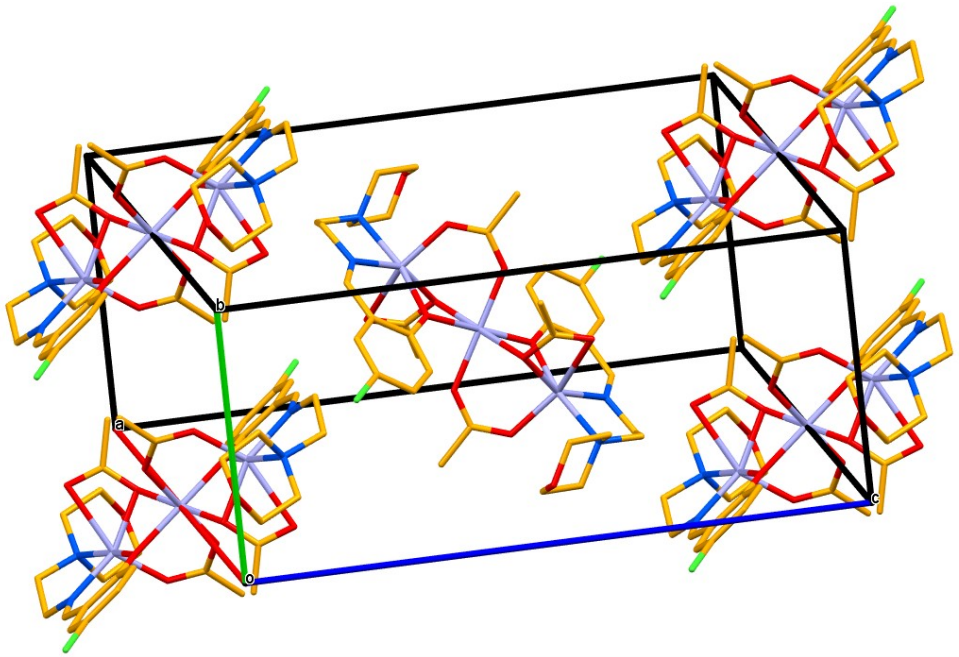

Fig. S3. Packing diagram of **C1**.

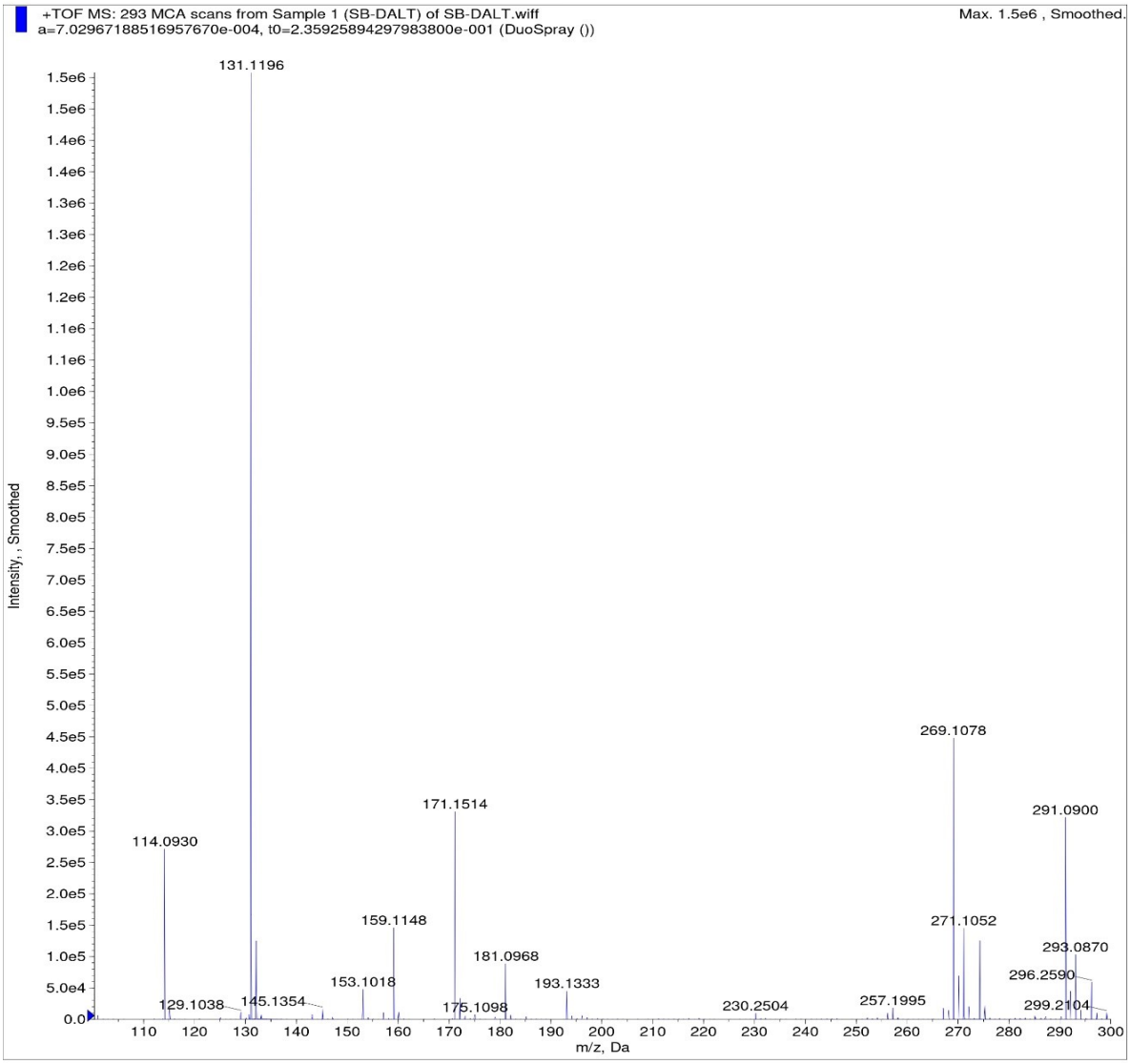

Fig. S4. Mass spectrum of ligand **L1.**

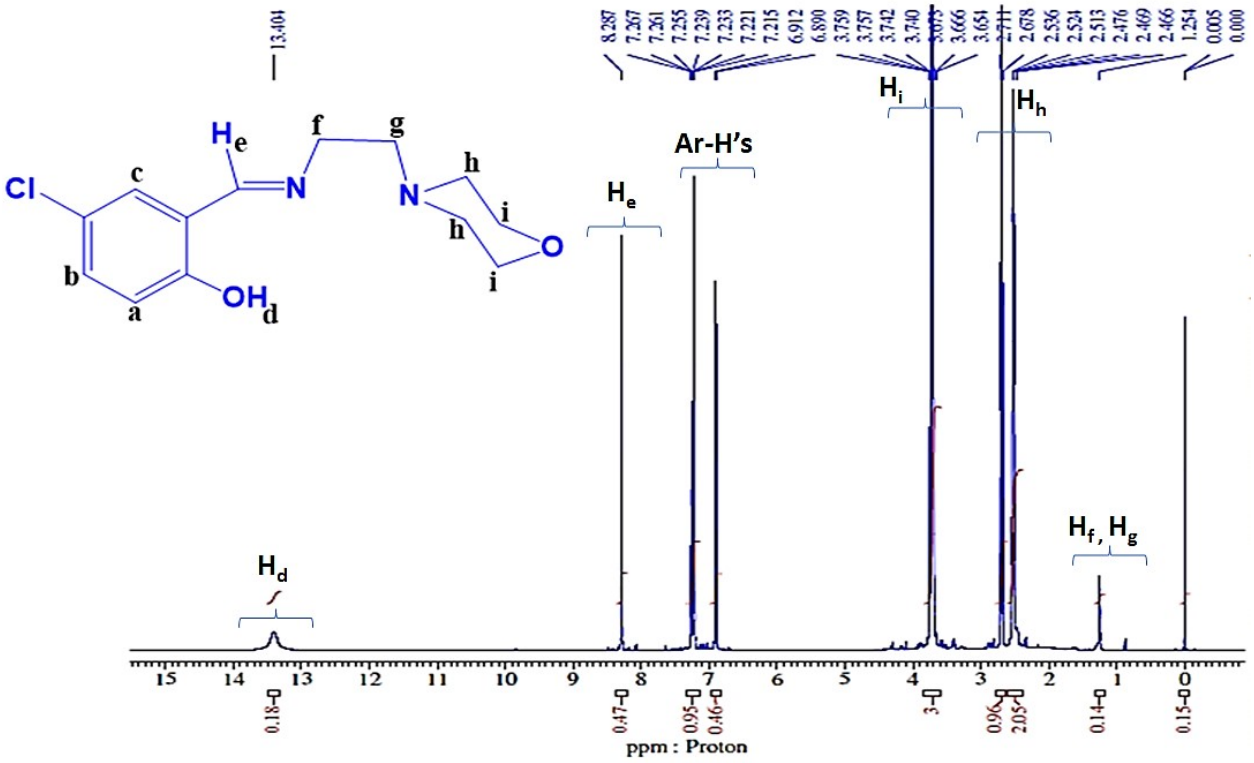

Fig. S5. [1]H NMR spectrum of **L1**.

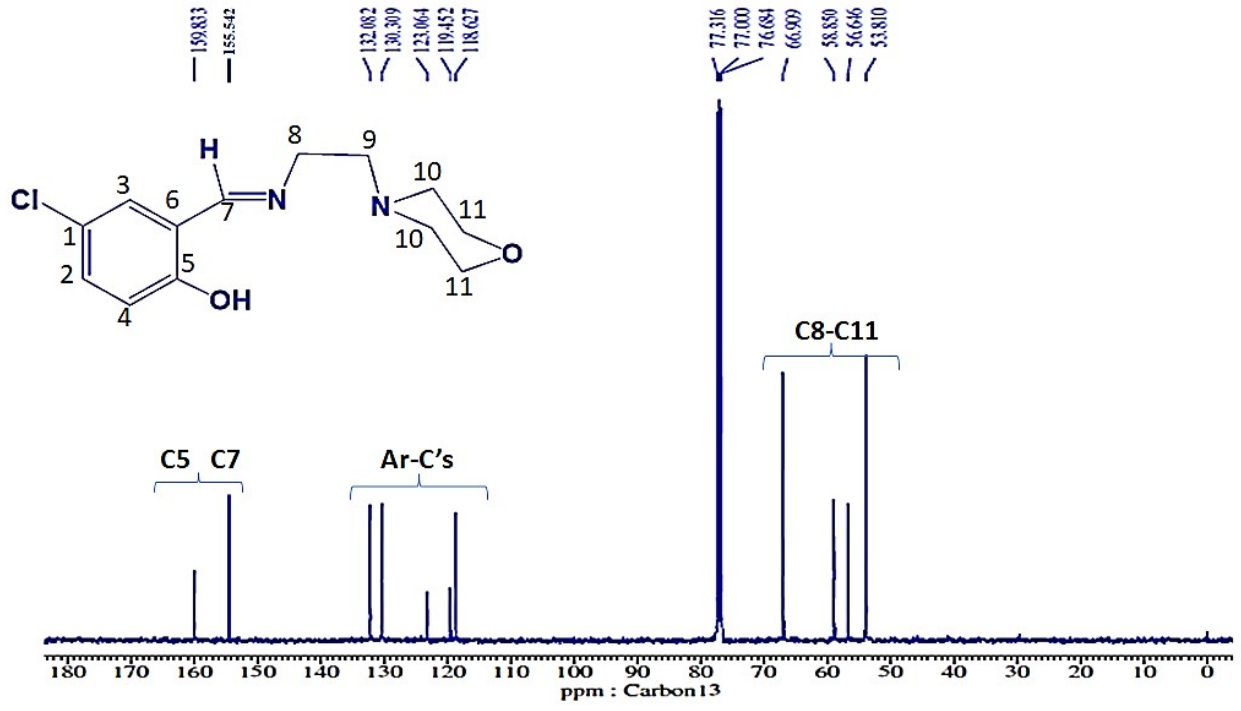

Fig. S6. [13]C NMR spectrum of **L1**.

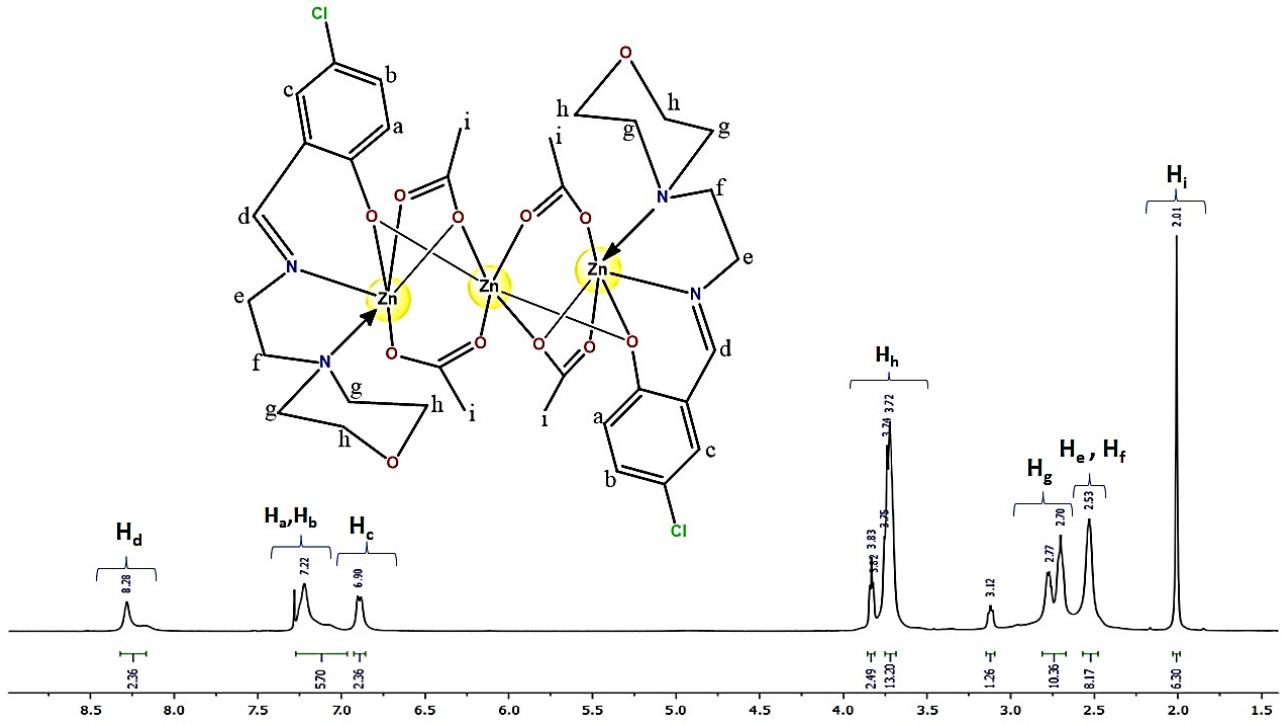

Fig. S7. ^{1}H NMR spectrum of **C1**.

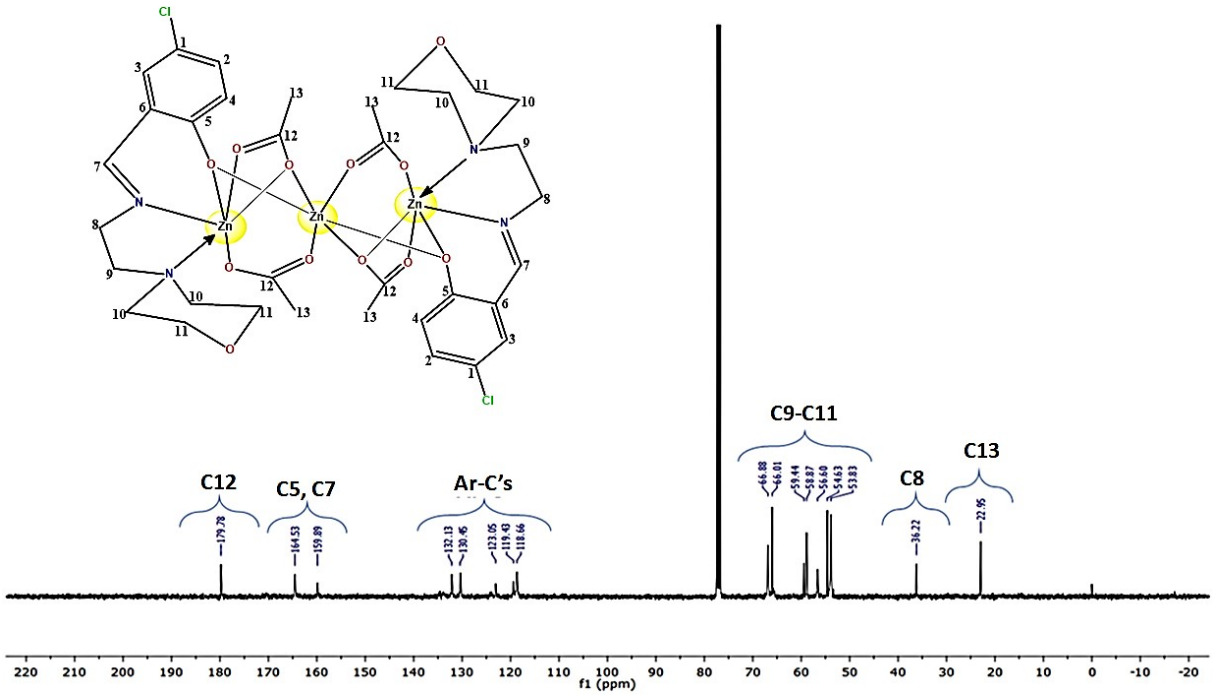

Fig. S8. ^{13}C NMR spectrum of **C1**.

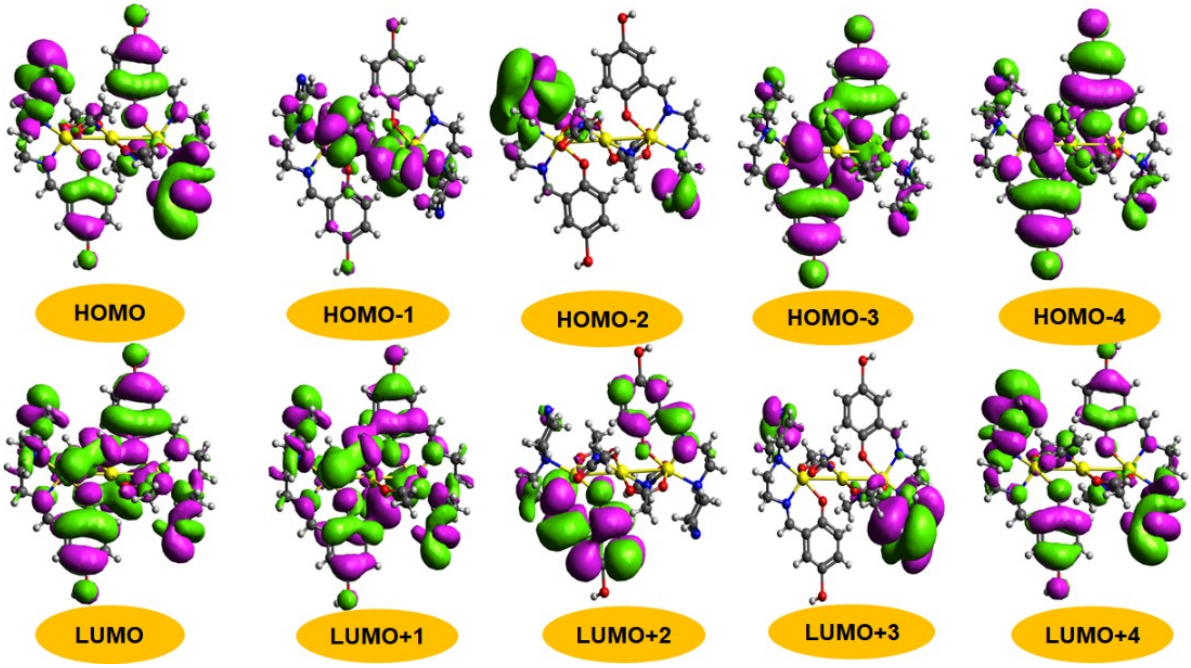

Fig. S9. DFT generated various FMOs of **C1** at B3LYP level.

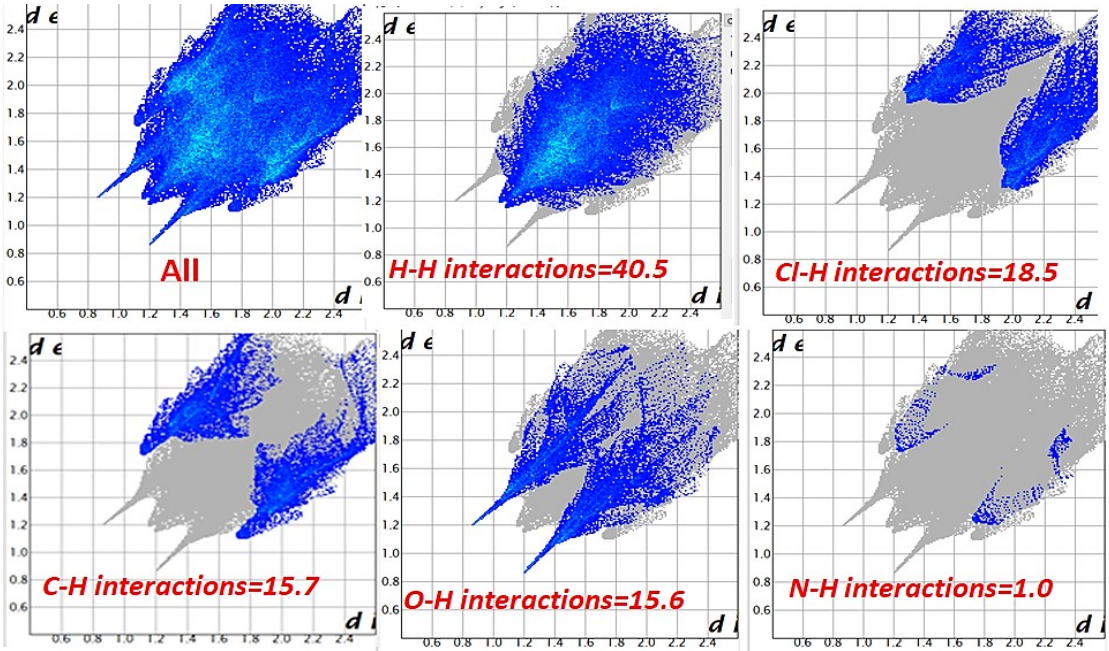

Fig. S10. Hirshfeld surface analysis of **C1** in 2D fingerprint plots.

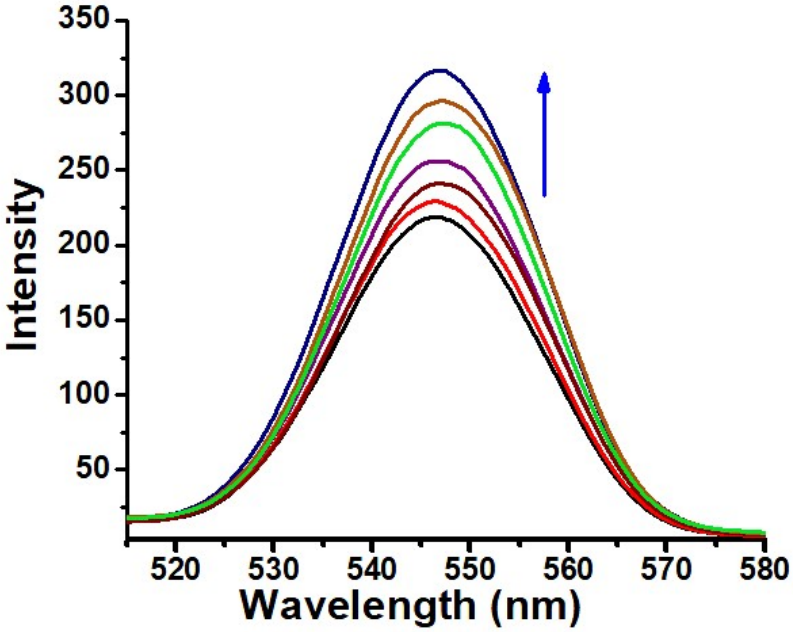

Fig. S11. Emission spectra of **C1** on increasing aliquots of ct−DNA. [**C1**] = 2.4 μM and [ct−DNA] = 0.1–0.7 μM.

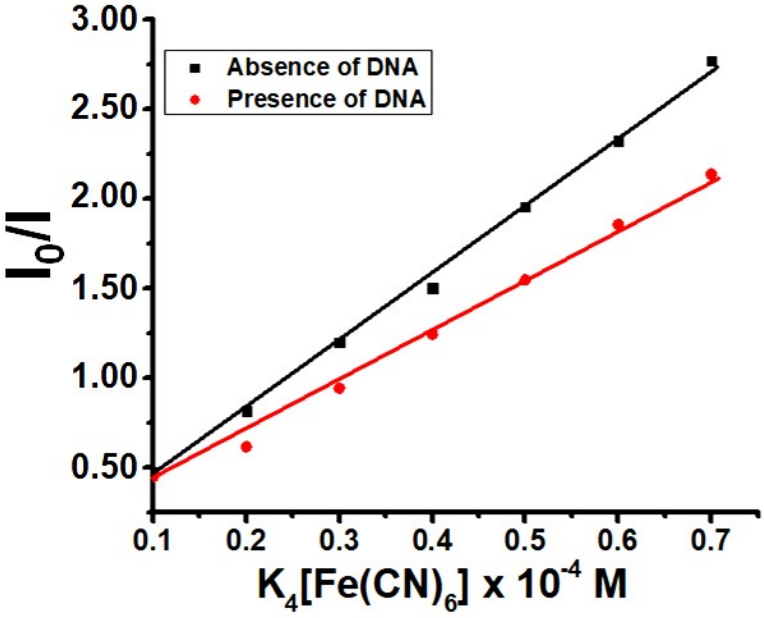

Fig. S12. Stern–Volmer quenching plots of **C1** with increasing concentration of $[Fe(CN)_6]^{4-}$ in the absence (Black) and in the presence (Red) of ct−DNA.

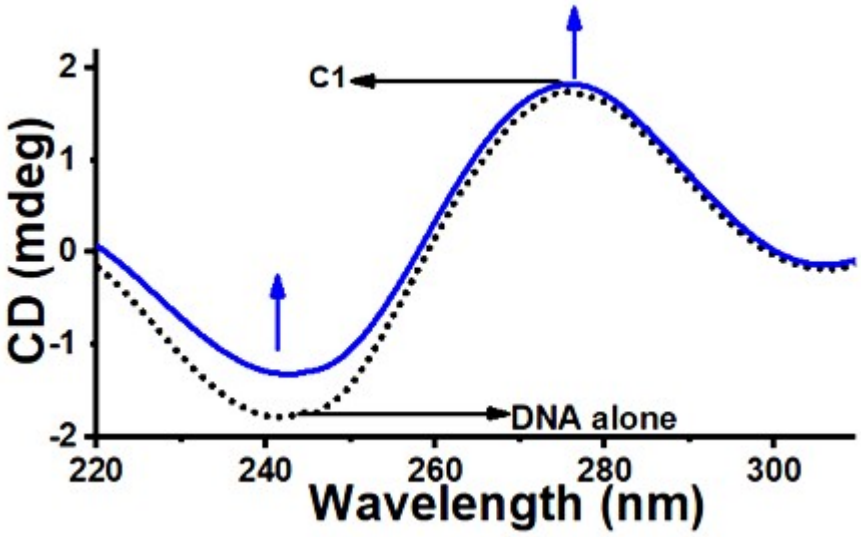

Fig. S13. Circular dichroism spectra of **C1** in presence and absence of DNA.

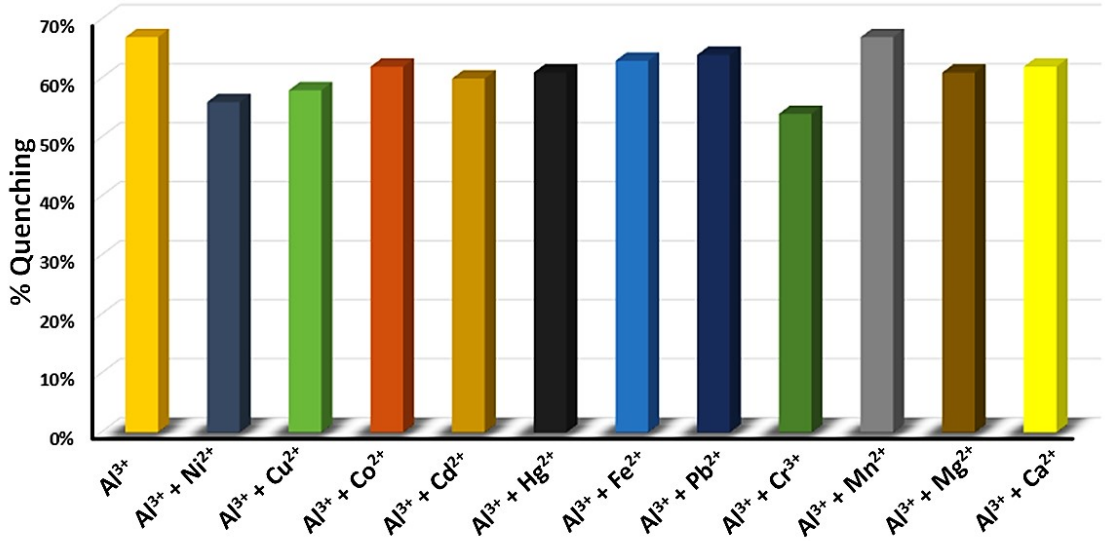

Fig. S14. Interference experiment of complex **C1** in presence of different co−interfering cations and Al^{3+} ion in buffer solution (pH =7.2).

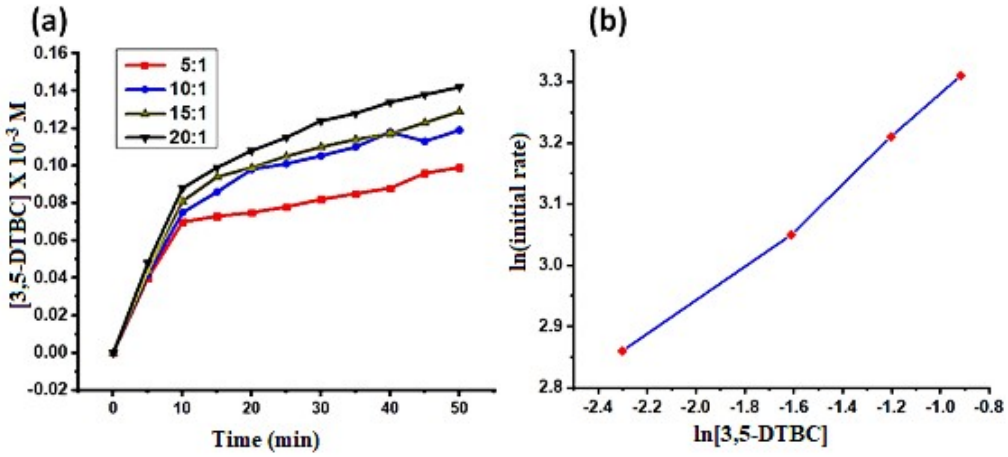

Fig. S15. (a) Plot of formation of product 3,5 [DBCQ] *vs* time while keeping catalyst (**C1**) concentration constant and (b) logarithmic plot between substrate (3,5−DTBC) concentration and initial rate.

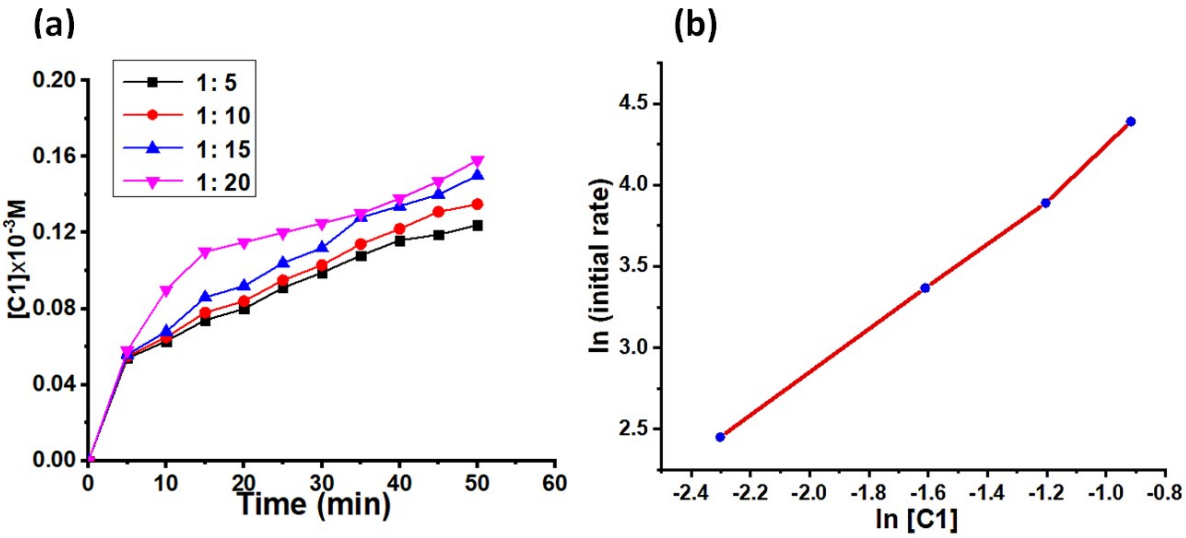

Fig. S16. (a) Plot of formation of product 3,5 [DTBQ] *vs* time while keeping substrate (3,5−DTBC) concentration constant and (b) logarithmic plot between catalyst (**C1**) concentration and initial rate.

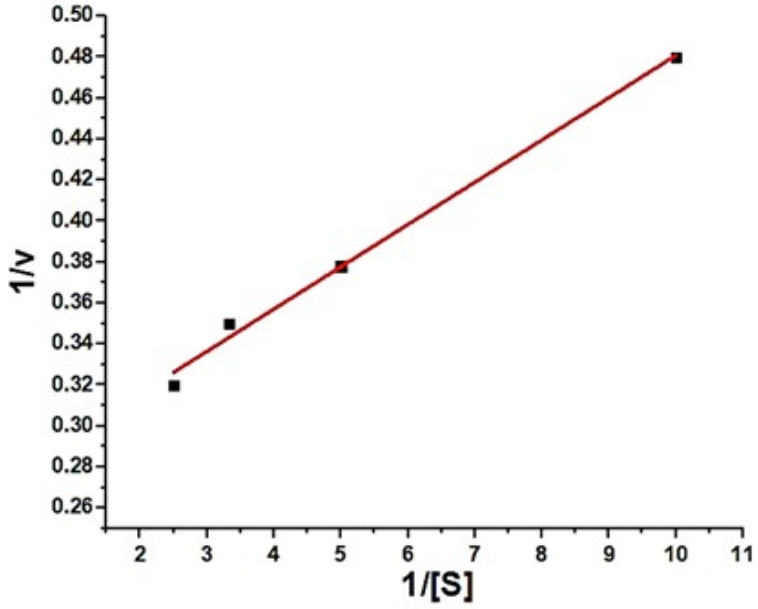

Fig. S17. Lineweaver−Burk plot (double reciprocal plot) for complex **C1**.

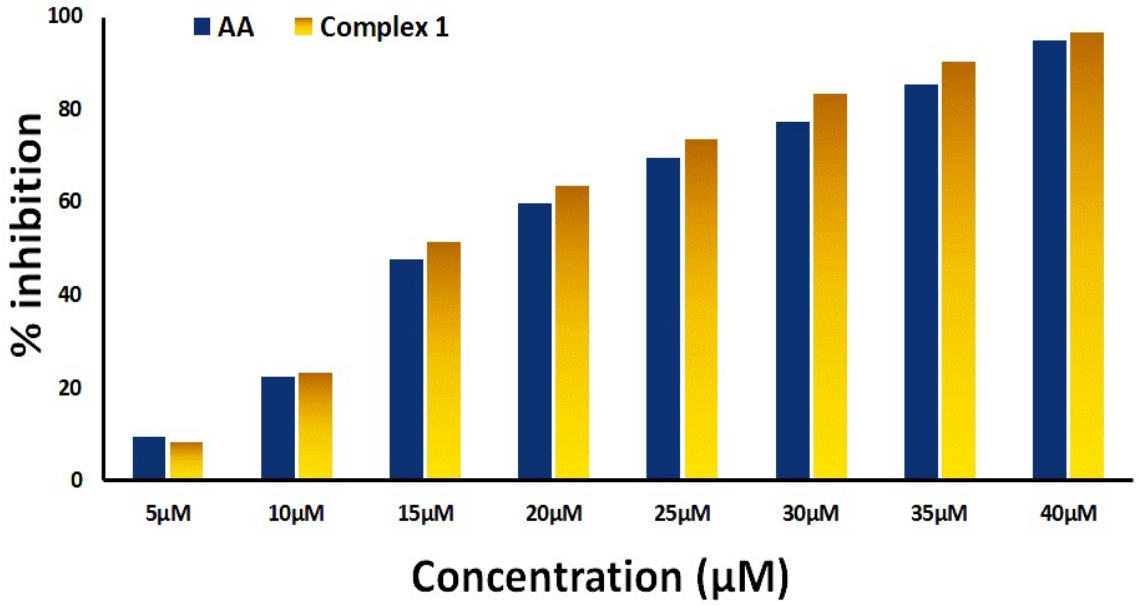

Fig. S18. Antioxidant activity of **C1** (yellow) along with **AA** (Blue) as a standard.

References

[S1] D. Dey, G. Kaur, A. Ranjani, L. Gayathri, P. Chakraborty, J. Adhikary, J. Pasan, D. Dhanasekaran, A. R. Choudhury, M. A. Akbarsha and N. Kole, *Eur. J. Inorg. Chem.,* 2014, **21**, 3350−3358.

[S2] S. Pal, B. Chowdhury, M. Patra, M. Maji, and B.Biswas, *Spectrochim. Acta A Mol. Biomol. Spectrosc.,* 2015, **144**, 148−154.